HHS Public Access

Author manuscript

Curr Biol. Author manuscript; available in PMC 2016 November 02.

Published in final edited form as:

Curr Biol. 2015 November 2; 25(21): 2751–2762. doi:10.1016/j.cub.2015.09.025.

Warts phosphorylates Mud to promote Pins-mediated mitotic spindle orientation in *Drosophila* independent of Yorkie

Evan B. Dewey, **Desiree Sanchez**, and **Christopher A. Johnston**

Department of Biology, University of New Mexico, Albuquerque, NM, 87131, USA

SUMMARY

Multicellular animals have evolved conserved signaling pathways that translate cell polarity cues into mitotic spindle positioning to control the orientation of cell division within complex tissue structures. These oriented cell divisions are essential for the development of cell diversity and the maintenance of tissue homeostasis. Despite intense efforts, the molecular mechanisms that control spindle orientation remain incompletely defined. Here we describe a role for the Hippo (Hpo) kinase complex in promoting Partner of Inscuteable (Pins)-mediated spindle orientation. Knockdown of Hpo, Salvador (Sav), or Warts (Wts) each result in a partial loss of spindle orientation, a phenotype previously described following loss of the Pins-binding protein Mushroom body defect (Mud). Similar to orthologs spanning yeast to mammals, Wts kinase localizes to mitotic spindle poles, a prominent site of Mud localization. Wts directly phosphorylates Mud *in vitro* within its C-terminal coiled-coil domain. This Mud coiled-coil domain directly binds the adjacent Pins-binding domain to dampen the Pins/Mud interaction, and Wts-mediated phosphorylation uncouples this intramolecular Mud interaction. Loss of Wts prevents cortical Pins/Mud association without affecting Mud accumulation at spindle poles, suggesting phosphorylation acts as a molecular switch to specifically activate cortical Mud function. Finally, loss of Wts in *Drosophila* imaginal disc epithelial cells results in diminished cortical Mud and defective planar spindle orientation. Our results provide new insights into the molecular basis for dynamic regulation of the cortical Pins/Mud spindle positioning complex and highlight a novel link with an essential, evolutionarily-conserved cell proliferation pathway.

INTRODUCTION

During cell division the mitotic spindle apparatus directs the localization of the actomyosin contractile ring and cleavage furrow ingression; thus, spindle positioning serves as an essential determinant of cell division orientation. Two fundamental aspects of animal development arise from this principle. First, spindle orientation directs the asymmetric

Address correspondence to: johnstca@unm.edu.

AUTHOR CONTRIBUTIONS

Conceptualization, C.A.J.; Formal Analysis, E.B.D. and C.A.J.; Investigation, E.B.D., D.S., and C.A.J.; Writing – Original Draft, C.A.J.; Writing – Review & Editing, C.A.J.; Visualization, E.B.D. and C.A.J.; Supervision, C.A.J.

segregation of cell fate determinants during stem cell divisions, providing a means of balancing self-renewal and differentiation. For example, uncoupling of spindle orientation from the cortical polarity axis in *Drosophila* neuroblasts can contribute to an overproliferation of these neural stem cells, disrupting proper CNS development and resulting in severe tissue overgrowth phenotypes [1, 2]. Second, the establishment and maintenance of complex tissue structures relies on spindle orientation in order to balance cell divisions that lead to tissue expansion versus stratification. For example, spindle orientation defects in the mouse epidermis result in defective stratification, yielding tissue structures that are incapable of proper fluid and electrolyte regulation [3]. Despite being linked to several developmental disorders and having recently emerged as a possible contributor to tumorigenesis [4], the molecular details of spindle orientation process remain incomplete.

The conserved Partner of Inscuteable (Pins) protein regulates spindle orientation in diverse cell types from model organisms spanning metazoan evolution and represents perhaps the best-characterized regulator of spindle positioning [5–9]. Pins is thought to control spindle orientation through two synergistic pathways: (1) its tetratricopeptide repeat (TPR) domains directly bind Mushroom body defect (Mud) to activate dynein-dependent spindle forces, and (2) its phosphorylated ‘Linker’ domain directly binds Discs large (Dlg) to capture microtubule plus ends through the kinesin motor protein Khc-73 [10, 11]. Mud/dynein-mediated forces generate rapid spindle oscillations to position the metaphase spindle prior to anaphase onset [6, 12]. Mud is a spindle pole/centrosomal protein that becomes cortically polarized in a Pins-dependent manner. Loss of Pins in *Drosophila* neuroblasts, which induces spindle orientation defects, prevents cortical Mud enrichment without affecting its spindle pole localization [13, 14]. Mud at spindle poles contributes to spindle assembly processes, whereas cortical Mud localization is essential for proper spindle positioning. Furthermore, cortical targeting of dynein-mediated forces appears to be sufficient for spindle orienting activity [12]. Together, these results suggest distinct Mud functions are elicited through differential subcellular localizations and highlight the importance of cortical localization in Mud-mediated spindle orientation. Recent studies have demonstrated Ran- and CDK1-dependent pathways that prevent cortical Mud association; however, the molecular mechanisms that promote the formation of cortical Pins/Mud remain largely undefined [15, 16].

Using a combination of biochemical, cellular, and genetic methods, we define a role for the Hippo kinase complex, an eminent regulator of cell growth and proliferation [17], in Pins/Mud-mediated spindle orientation. The core complex components Hippo (Hpo), Salvador (Sav), and Warts (Wts) are each required for spindle orientation to a cortically polarized Pins cue. RNAi directed against individual Hpo components results in a partial loss of spindle orientation, a unique phenotype previously described following selective loss of the Mud/dynein arm of Pins signaling. Wts localizes to mitotic spindle poles and directly phosphorylates Mud *in vitro* within its terminal coiled coil (Mud^{CC}) domain. We also show that Mud^{CC} directly interacts with the adjacent Pins-binding domain (Mud^{PBD}) to regulate its Pins binding capacity. Wts phosphorylation prevents this putative intramolecular interaction, suggesting Wts functions to enhance Pins/Mud complex formation. Consistent

with this, loss of Wts prevents Pins-mediated cortical Mud accumulation without perturbing its accumulation at spindle poles. Finally, Wts-directed RNAi results in defective Mud localization and a loss of planar spindle orientation in *Drosophila* imaginal wing disc epithelial cells. Together, our results demonstrate a novel mode of regulating Pins/Mud-dependent spindle orientation through the Hippo tumor suppressor pathway, highlighting an important intersection between cell cycle and spindle orientation pathways.

RESULTS

Warts and Mud localize to spindle poles in mitotic S2 cells

To identify molecular pathways that promote polarized cortical Mud localization, we reasoned that proteins localized to mitotic spindle poles with cell cycle-dependent activity would represent attractive candidates. The Hippo kinase complex localizes to spindle pole bodies (SPB) in *S. cerevisiae* (the yeast equivalent of centrosomes), and its activity increases throughout mitosis to ultimately induce anaphase onset and mitotic exit through the Mitotic Exit Network (MEN) signaling system [18, 19]. Interestingly, Cdc15 (the yeast Hippo ortholog) activity is necessary for proper orientation of the mother SPB into the nascent bud cell; however, this effect is mediated through asymmetric activity of centrosomal Kar9, a protein with no apparent metazoan ortholog [20]. MEN activity is dependent on spindle pole body activity of Dbf2, the yeast equivalent of Wts. Studies using both mouse and human cell culture systems have confirmed that components of the Hippo complex, in particular the Wts kinase orthologs LATS1/2, also localize to spindle poles/centrosomes where they control centrosome disjunction, chromosome segregation, and cell cycle progression [21–26]. We have thus focused herein on the role of Hippo signaling in oriented cell division using *Drosophila* as a model system.

We first examined the cellular localization of Wts, the key kinase output in Hippo signaling, in *Drosophila* S2 cells. We cloned full-length Wts from an S2 cDNA library, indicating this gene is endogenously transcribed, and expressed low amounts as a FLAG-tagged transgene. As shown in Figure 1, FLAG-Wts localized to mitotic spindle poles, including proximal regions of their emanating microtubules. This localization in S2 cells is identical to that seen with endogenous Mud (Figure 1). We further examined Mud and Wts localization following colchicine-induced microtubule depolymerization. Colchicine treatment resulted in primarily cytoplasmic localization of both Mud and Wts with no significant localization at γ-tubulin positive centrosomes, consistent with localization specifically to spindle poles and proximal spindle microtubules. These results are in agreement with previous studies of Mud localization [27]. We conclude that Wts kinase localization resembles that of Mud both spatially and temporally at mitotic spindle poles.

Hippo kinase signaling is required for Pins-mediated spindle orientation

We next investigated whether the Hippo complex regulates spindle positioning in S2 cells using an ‘induced polarity’ reconstitution assay [10]. Cells were transfected with the cell adhesion molecule Echinoid (Ed) fused to Pins at its intracellular C-terminus (Ed:Pins), which localizes specifically to sites of cell-cell contact, thus generating Ed-dependent cortical polarization of Pins in an otherwise non-polarized cell. Spindle orientation is then

measured relative to these induced polarity crescents within small, otherwise isolated clusters (2–3 cells) containing one contiguous patch of Ed:GFP signal (Figure 2A). As previously reported, the mitotic spindle exhibits robust alignment to the center of this Ed:Pins crescent, whereas cells expressing Ed alone display random spindle orientation (Figure 2C). Also consistent with our previous studies, treatment of cells with RNAi directed against Mud resulted in a partial loss of Ed:Pins-mediated spindle orientation, intermediate between the effects of Ed:Pins and Ed (Figure 2B,C). This partial loss-of-function phenotype contrasts with the complete dysfunction induced by Dlg^{RNAi}, and is the result of attenuated dynein-mediated spindle forces [10]. Individual RNAi treatments against Hpo, Sav, or Wts each caused a partial loss of spindle orientation phenotype that was statistically indistinguishable from Mud^{RNAi}, which can be seen in representative images (Figure 2B) as well as when expressed as a cumulative percent across the entire sample of cells collected (Figure 2C). To control for potential off-target effects, we designed two additional RNAi sequences for each Hippo component that targeted distinct regions of their coding sequences. These alternative RNAi treatments all produced phenotypes identical to the initial results, suggesting that off-target effects were unlikely (Figure S1). We also quantified spindle orientation relative to the outer edge of the Ed:Pins crescent; whereas control cells preferentially orient spindles to the crescent center, a tighter coupling between spindles and the crescent edge is observed following RNAi against Hpo, Sav, or Wts, a result that also mirrors the effects of Mud^{RNAi} (Figure 2D). This phenotype is consistent with residual activity of the spindle-capturing Dlg/Khc-73 pathway, which can operate in the absence of the Mud/Dynein pathway, and suggests that the core Hippo complex is dispensable for Dlg/Khc-73 function [10]. Thus, these results suggest that the Hpo/Sav/Wts complex functions specifically within the Pins/Mud/dynein spindle orientation pathway and serves as a positive modulator of its activity.

Wts is a member of the NDR (nuclear Dbf2-related) protein kinase family, which also includes the evolutionarily-conserved NDR1/2 kinase, Tricornered (Trc) [28]. Despite strong primary sequence homology and identical consensus phosphorylation target motifs, Trc participates in functions distinct from Wts. Trc localizes to the cytoplasm and cell cortex and maintains extended cellular structures, such as epidermal hair and dendritic branches in sensory neurons [29]. As knockdown of kinases could have pleiotropic effects, we reasoned that Trc would serve as an ideal negative control. Indeed, Trc^{RNAi} treatment did not significantly alter Ed:Pins-mediated spindle orientation (10.4 ± 6.2, n=49 compared to 11.0 ± 14.5, n=47 with Trc^{RNAi}), consistent with a Wts-specific regulation of Pins/Mud function in S2 cells.

Hippo signaling controls spindle orientation independent of Yorkie

The canonical phosphorylation target of Wts kinase is the transcriptional regulator, Yorkie (Yki), which normally promotes cell cycle progression through upregulation of genes such as c-myc and cyclin-E [30, 31]. Yki phosphorylation, however, prevents its nuclear translocation and function, resulting in cytoplasmic retention thereby explaining the growth suppressive effects of canonical Hpo pathway [32]. As Wts^{RNAi} treatment would be predicted to increase Yki activity, we designed two approaches to assess whether elevated Yki function may contribute to spindle orientation defects following loss of Wts. First, we

simultaneously treated cells with both Wts^{RNAi} and Yki^{RNAi} to determine if Yki^{RNAi} could suppress Wts^{RNAi}-mediated effects. However, as shown in Figure 3B, combined RNAi against Wts and Yki did not differ from Wts^{RNAi} alone. Treatment of cells with Yki^{RNAi} alone did not perturb Ed:Pins function either, indicating Yki is also not necessary for spindle orientation. Combined treatment with Wts^{RNAi} and Mud^{RNAi} did not differ from treatment with either alone (Figure 3B), adding further support that Wts functions together with Mud to regulate spindle orientation. Second, we overexpressed a constitutively active, 'phosphodead' Yki mutant (Yki^{S168A}) and monitored for a potential dominant phenotype. Yki^{S168A} expression did not significantly affect Ed:Pins-mediated spindle orientation, however. As a complementary approach, we also overexpressed the Yki target gene cyclin-E as another means of mimicking the possible effects of enhanced Yki activity. As with Yki itself, cyclin-E overexpression did not significantly alter spindle orientation (Figure 3A,B). Conditions leading to reduced Wts or Mud function again resulted in precise alignment to crescent edges, whereas cells with compromised Yki function remained oriented preferentially to the middle of Ed:Pins crescents (Figure 3C). These results collectively suggest that the effects of Wts^{RNAi} on spindle orientation are Yki-independent and likely act through an alternative, 'non-canonical' pathway.

Warts directly phosphorylates Mud at its C-terminal coiled-coil domain

Spindle pole localization at metaphase, the phenocopy of Mud^{RNAi} treatment, and the lack of Yki-dependent effects all lead us to explore the hypothesis that Wts functions directly within the Mud pathway. Wts is a serine/threonine kinase that preferentially phosphorylates the consensus sequence motif H-x-R/K-x-x-S/T (where 'H' represents Histidine, 'R/K' represent Arginine/Lysine, and 'x' represents any amino acid) [33]. Although basic residues at the −2 and/or −3 positions are characteristic of several protein kinase families, the histidine at −5 is the signature preference of the Wts recognition motif, although its presence may not be absolutely mandatory. Using the Eukaryotic Linear Motif (ELM; http://elm.eu.org/) program, we performed *in silico* analyses of Pins/Mud pathway components [11], revealing a single, strongly predicted Wts phosphorylation site within Mud itself. This site lies within the C-terminal Mud coiled-coil domain (Mud^{CC}) at serine-1868 (S1868; Figure 4A). To directly examine this prediction experimentally, we cloned and purified the Mud^{CC} domain to homogeneity (Figure 4D) and qualitatively examined phosphorylation using an [γ-32P]-ATP radiometric kinase assay with purified Wts. As shown in Figure 4B, Wts directly phosphorylated Mud^{CC}. A single alanine substitution at the predicted phosphorylation site (S1868A) completely abolished the detected signal. These results demonstrate that S1868 in the Mud^{CC} domain is a direct *in vitro* substrate of Wts kinase.

The mitotic functions of Mud, particularly those of the cortical Pins/Mud complex, appear to be evolutionarily conserved, yet the overall primary sequence conservation across Mud orthologs is remarkably low [13, 14]. Sequence comparison between orthologous Mud^{CC} domains specifically, however, reveals that Wts phosphorylation is likely to be a conserved regulatory mechanism (Figure S3). NuMA, the mammalian Mud ortholog, contains numerous predicted phosphorylated sites [34], and the NuMA C-terminal coiled-coil domain ($NuMA^{CC}$) in several vertebrates (including humans) retains both the S/T phospho-acceptor residue and the conserved R/K in the −3 position (Figure S1). The histidine at the −5

position preferred within the Wts motif is not conserved, although other Wts substrates have been identified that violate this sequence rule as well [35]. Radiometric kinase assays demonstrated that NuMA is indeed a direct Wts substrate, with a single T1677A mutation greatly reducing phosphorylation (Figure 4C). Furthermore, MARCOIL sequence analysis (Max-Planck Institute for Developmental Biology) revealed that the coiled-coil register is identical between Mud^{CC} and $NuMA^{CC}$, with the phosphorylated S/T residue residing at a surface exposed 'E-position' in both (Figure 4F), and, like Mud^{CC}, $NuMA^{CC}$ is predicted to exist as a trimer. Size exclusion chromatography confirmed the trimeric nature of both Mud^{CC} and $NuMA^{CC}$ purified proteins (Figure 4E). These results highlight structural conservation between fly and human orthologs of this key coiled-coil domain. Among *Drosophila* Mud isoforms themselves, it is interesting to note that the Mud^{PBD} and Mud^{CC} domains are mutually inclusive. Specifically, the solitary Mud^{PBD}-containing isoform, expressed in neuroblasts and likely other cells undergoing Pins-dependent oriented divisions, contains Mud^{CC}, whereas the other two distinguished isoforms exclude Mud^{CC} by sequence truncation or alternative splicing [14].

Phosphorylation of Mud^{CC} prevents its self-association with Mud^{PBD}

To understand the impact of Wts on Mud function, we next explored how phosphorylation might affect Mud structure. The Mud^{CC} domain was originally identified as part of the Pins binding region and immediately precedes the minimal Pins binding sequence subsequently described [13, 14, 36], referred to as Mud^{PBD} herein (Figure 4A). Sequence analysis of the Mud^{CC} and Mud^{PBD} domains revealed significantly opposing surface charge potentials, with predicted isoelectric points of 9.4 and 4.4, respectively (ExPASy Bioinformatics Resource Portal), leading us to speculate that these adjacent domains may exist in an intramolecularly bound conformation. To test this model, we purified the isolated Mud^{PBD} as GST-fusion protein, immobilized it on glutathione agarose beads, and performed 'pulldown' assays with purified Mud^{CC} as an isolated, soluble Mud fragment. Indeed, Mud^{CC} interacted directly with Mud^{PBD} as an *in trans* complex (Figure 5A,B). We then examined whether Wts might modulate this interaction. Phosphorylation of Mud^{CC} by Wts abolished its ability to bind Mud^{PBD} (Figure 5A). These results suggest that Mud exists in an intramolecular conformation through Mud^{CC}-Mud^{PBD} association, a structural feature which is negatively regulated by Wts kinase activity (Figure 5D).

We next considered whether Mud^{PBD} binds Mud^{CC} using similar sequence elements used to bind the TPR domains of Pins [36]. Based on the crystal structure of the LGN/NuMA complex (the mammalian Pins/Mud orthologs), we designed a double charge-reversal (E1939K/E1941K; "EEKK") mutation in Mud^{PBD}. These two residues are strictly conserved between Mud and NuMA, contribute significantly to the LGN/NuMA interaction, and represent strong candidate amino acids to respond to introduction of a negatively charged phosphate on Mud^{CC}. As shown in Figure 5B, this Mud^{PBD} mutant was dramatically impaired in its ability to bind Mud^{CC}. These results are consistent with an electrostatic model of Mud^{CC}-Mud^{PBD} association and suggest that this intramolecular Mud interaction could mask key Pins binding residues, possibly serving as a mode of Mud autoinhibition.

To test whether the intramolecular Mud interaction affects its ability to directly interact with Pins *in vitro*, we examined binding of $Pins^{TPR}$ to either Mud^{PBD} alone or the $Mud^{CC\text{-}PBD}$ tandem domain cassette as GST fusion proteins. Binding of $Pins^{TPR}$ to Mud^{PBD} was detectable at low Pins concentrations and fit to a normal Langmuir binding model. In contrast, interaction with $Mud^{CC\text{-}PBD}$ was significantly reduced specifically within a low $Pins^{TPR}$ concentration regime, with the binding curve displaying a slightly steeper slope than seen with Mud^{PBD} alone (Figure 5C). These data indicate that the proximal Mud^{CC} domain suppresses the formation of the Pins/Mud^{PBD} complex at low concentrations and may shape the overall dynamics of the interaction. We speculate this may function to prevent unproductive Pins binding at sites of low expression such as the spindle proximal cytoplasm, thus aiding in the productive formation of a cortical Pins/Mud complex (Figure 5D).

Warts is required for cortical but not spindle pole Mud localization

To understand how the Wts/Mud interaction might impinge upon Mud function within a cellular context, namely with respect to its association with Pins, we visualized endogenous Mud localization in S2 cells. In cells with induced Ed:Pins cortical polarity, Mud localizes strongly to both spindle poles as well as accumulating at the cortical Pins crescent (Figure 6), similar to that seen *in vivo* [3, 13, 14]. Treatment with Wts^{RNAi} resulted in a significant reduction in cortical Mud signal; however, its localization to spindle poles was largely unaffected by Wts loss-of-function (Figure 6). Together with the *in vitro* binding experiments above, these data indicate that Wts-mediated Mud phosphorylation serves as a positive cortical localization signal.

Warts facilitates Mud-dependent spindle orientation in *Drosophila* wing disc epithelia

The Hippo signaling pathway is well known to regulate cell proliferation and tissue size *in vivo* through its inhibitory action on Yki [17]. Recent studies suggest that this pathway also controls the orientation of cell division in the *Drosophila* imaginal wing disc, a tissue in which planar polarized Fat-Dachsous, an upstream activator of Hpo [37, 38], instructs directional tissue growth by controlling orientation of individual cell divisions [39, 40]. Mechanisms proposed for this function include proliferation-induced cell crowding and modulation of the actin cytoskeleton, leading to mechanical forces that alter cortical tension and cell shape globally throughout the tissue [41, 42]. Both of these models implicate tissue-level mechanics that determine mitotic orientations and have been suggested to operate through canonical Wts/Yki activity [43]. Our results in small, Ed-induced S2 cell clusters, a minimal reconstitution system less constrained by tissue-dependent signaling, suggests Wts may exert cell intrinsic effects as well, independent of Yki-dependent growth. Such activity could operate via regulation of Mud, which has recently been shown to regulate oriented divisions in wing disc epithelia as well [44]. We expressed hairpin *UAS*-RNAi sequences directed against Mud or Wts using the *nubbin*-GAL4 (nub^{GAL4}) driver that expresses throughout the wing disc pouch. Mitotic orientations relative to the wing disc axis fluctuate based on cell position within the tissue [41, 45]; thus, we chose to quantify spindle orientation relative to adjacent actin rich folds typical of late larval discs (Figure 7A). In this paradigm, cells from control animals showed a nearly perfect bias for spindle orientation parallel to the overlaying actin fold. Mud^{RNAi} expression significantly attenuated this bias,

resulting in more randomized spindle orientations (Figure 7A,B), consistent with similar studies reported recently [44, 46]. Expression of RNAi against Hpo, Sav, or Wts each resulted in a nearly identical loss of spindle orientation, suggesting these genes may function in a linear pathway to control oriented epithelial divisions (Figure 7A,B). We also examined spindle orientation in wing discs expressing Wts^{RNAi} driven by two alternative GAL drivers, *apterous*-GAL4 and *engrailed*-GAL4. Both of these conditions resulted in a loss of spindle orientation similar to that seen with *nubbin*-GAL4 (Figure S3). It should be noted that the *nubbin*-GAL4 stock contains UAS-Dicer2 on its X-chromosome; however, its presence did not significantly enhance the effects of Mud^{RNAi} on the spindle orientation phenotype (Figure S4). To test whether Wts^{RNAi} expression alters Mud function, we examined Mud localization in dividing epithelial cells. In control wing discs, Mud localized strongly to both spindle poles as well as the cell cortex, with a bias towards cortical regions above each spindle pole. In contrast, cells from Wts^{RNAi}-expressing discs showed a significant reduction of cortical Mud signal, although Mud localization at spindle poles was not significantly affected (Figure 7C,D). These results mirror those obtained in S2 cells and implicate Wts as an essential determinant of cortical Mud localization and a positive regulator of the Pins/Mud spindle positioning complex in epithelial cells. Cortical actin was not altered under any conditions tested (Figure 7D). We also examined localization of Pins, which although implicated in asymmetric division of wing disc sensory organ precursor cells [5, 47], has not been directly investigated in disc epithelial cells to our knowledge. Pins was cortically localized and accumulated at regions above spindle poles, similar to that seen with Mud. In contrast to Mud, however, expression of Wts^{RNAi} did not significantly affect Pins cortical association (Figure 7E), consistent with a model in which Wts is required for Mud recruitment to an independently-established cortical Pins cue.

Mud^{RNAi} alone did not cause significant defects in wing disc development (Figure 7F), similar to previous reports [44, 48]. Somewhat surprisingly, Hpo, Sav, and Wts RNAi expressions also did not induce significant tissue overgrowth in wing discs, suggesting that, under the expression conditions used, these constructs were not sufficient to induce excessive Yki activation despite the detrimental effects on spindle orientation (Figure 7F). The lack of overgrowth was independent of GAL4 driver (Figure S3), suggesting the Wts^{RNAi} construct being expressed was not completely penetrant with respect to regulation of tissue size. We therefore tested an alternative RNAi stock (Wts^{RNAi}-VDRC). nub^{GAL4}-mediated expression of this Wts^{RNAi}-VDRC did cause tissue overgrowth, as well as defective spindle orientation similar to the original Wts^{RNAi} stock (Figure 7B,F). That spindle orientation deficits are nearly identical in discs from both Wts RNAi lines despite dramatic differences in tissue growth suggests that, although both are influenced by Wts, these events may operate independent of one another (Figure 7G), although we cannot directly rule out possible differences in RNAi efficacy. To more directly examine the effects of hyperactive Yki on spindle orientation, we overexpressed the constitutively active, Wts-insensitive Yki^{S168A} mutant, which induced a marked overgrowth phenotype (Figure 7F). Despite this misshapen tissue development, however, individual cell divisions remained oriented similar to those in wild-type discs (Figure 7A,B). Cortical Mud localization was also unaffected by Yki^{S168A} expression, again supportive of a Yki-independent Wts/Mud pathway (Figure 7C,D). Thus, Wts appears to regulate both the rate and orientation of cell

divisions through distinct downstream effectors with nonequivalent functions in these processes (Figure 7G). Specifically, phosphorylation of Yki imparts an inhibition of cell proliferation and tissue growth, while Mud phosphorylation acts as an activation of an essential spindle orientation mechanism. To further test this possibility, we examined wing discs of larvae expressing both Mud^{RNAi} and Yki^{S168A}. It should be noted that double mutant animals contain two UAS sequence elements, the same as when each was examine individually due to the selective presence of UAS-Dcr2 in single mutants. The phenotype of these Mud^{RNAi}/Yki^{S168A} double mutant discs appeared to be complementary. That is, discs remained overgrown as seen in the Yki^{S168A} alone; however, co-expression of Mud^{RNAi} induced a spindle orientation defect very similar to Mud^{RNAi} alone (Figure 7). Interestingly, Mud^{RNAi}/Yki^{S168A} double mutant discs experienced a significant ~33% reduction in size compared to Yki^{S168A} single mutant discs that show an overgrowth phenotype alone (Figure 7F), indicating that defective spindle orientation may limit overgrowth potential of this tissue.

DISCUSSION

In this study, we have identified a role for the core Hippo kinase complex in Pins/Mud-dependent spindle orientation (see Figure S5 for summary model). Warts kinase directly phosphorylates Mud within its C-terminal coiled-coil domain, which uncouples self-association with the adjacent Pins-binding domain, thus promoting formation of the Pins/Mud complex *in vitro*. Warts is required for cortical Mud localization and spindle orientation in cultured S2 cells as well as epithelial cells in *Drosophila* imaginal wing discs. Notably, this spindle orientation function of Warts is independent of the canonical pathway effector Yorkie. Thus, in addition to its well defined role in cell growth and proliferation through Yorkie inhibition, the Hippo pathway can also control the orientation of cell division through a novel Warts effector, Mud. The ability to coordinate the rate and orientation of mitotic events could have important impacts on tissue development and homeostasis.

Controlling the orientation of cell division is an essential underlying mechanism for cell diversification and tissue homeostasis in multicellular animals. Recent years have witnessed an impressive expansion in the identification of spindle orientation regulators [11]. The highly conserved Pins/Mud complex regulates spindle positioning in diverse cell types across animal taxa [49]; yet, the molecular mechanisms that regulate Pins/Mud activity remain sparsely defined. Using a human cell culture system, Kiyomitsu and Cheeseman recently showed that elevated activity of Ran-GTP localized at condensed metaphase chromosomes inhibited cortical localization of LGN/NuMA (human orthologs of Pins/Mud) [15]. This inhibitory signal prevents accumulation at the lateral cortex, indirectly permitting polarized localization that maintains spindle positioning. Kotak, et al. identified CDK1 as an additional negative regulator of cortical NuMA localization. CDK1-mediated phosphorylation reduces cortical NuMA in early phases of the cell cycle to prevent excessive spindle forces, whereas reduction in CDK1 activity at anaphase allows increased NuMA-mediated dynein activation necessary for spindle elongation [16]. As these two pathways dampen cortical Mud localization, what signals then promote the assembly and function of the cortical Pins/Mud complex?

Little is known about how Mud becomes cortically enriched specifically in polarized cells (*e.g*. with Pins). The Pins-binding protein Canoe (Cno) has been shown to be required for cortical Mud localization, although the molecular mechanism has not been thoroughly addressed [50, 51]. Cno itself localizes with apical Pins in dividing *Drosophila* neuroblasts, which is dependent on a network of monomeric G-proteins. Cno directly interacts with $Pins^{TPRs}$, which also serve as the binding site for Mud and Inscuteable (Insc). While recent studies have demonstrated that Mud and Insc bind competitively to $Pins^{TPRs}$ [36, 52], it remains to be determined whether similar Pins-binding dynamics exist with between Mud and Cno complex and how the $Pins^{TPRs}$ can accommodate such overlapping demand for its protein-protein interaction capacity. Phosphorylation, particularly in response to cell cycle commands, represents an attractive model for regulating such combinatorial protein interactions.

Another recent study demonstrated that a complex between the centriole duplication protein, Ana2, the dynein light chain molecule, Ctp, was necessary for cortical Mud localization in *Drosophila*. The Ana2/Ctp complex localized at spindle poles, and disrupting its expression prevented polarized cortical Mud association with Pins leading to improper spindle orientation [53], a phenotype strikingly similar to that observed herein following knockdown of the Hpo/Sav/Wts complex. Our *in vitro* binding experiments show that phosphorylation of the Mud coiled-coil domain abolishes a self-association with the Pins-binding domain, allowing for an increased Pins/Mud interaction affinity (Figure 5). Whether Mud phosphorylation affects its association with the Ana2/Ctp complex, directly or indirectly through an additional Mud-binding protein, and how this might impact this proposed mode of cortical Mud localization remains to be investigated.

The Hippo/Warts kinase pathway is a prominent regulator of cell proliferation and growth, yet a considerable amount of attention has been focused on Yki (and its transcriptional control of growth-associated genes) as the terminal pathway effector; noncanonical pathway effectors have only begun to emerge [54]. Our studies identify Mud as a novel target of Hpo/Wts signaling and provide evidence that Mud-dependent spindle positioning is controlled by this conserved kinase module. Upon mitotic entry, Hpo triggers NEK2-mediated centrosome dysjunction and bipolar spindle assembly [23]; our results suggest Hpo signaling persists in later phases of mitosis to regulate the positioning of this bipolar mitotic spindle. Thus, the Hpo complex appears to link cell cycle progression, primarily through regulation of G1/S promoting genes, with dynamic aspects of the mitotic spindle during M-phase. Elevated Hpo signaling at interphase suppresses cell growth and division, suggesting Hpo activation must be tightly regulated both spatially and temporally during M-phase transition. A diverse set of upstream regulators of Hpo function are beginning to be revealed, including cell adhesion and G-protein coupled receptors, cell polarity complexes, and the actin cytoskeleton [38], and further work will be required to identify possible activators of the spindle-associated Wts activity involved in spindle positioning. Perhaps more clear is the ability of diverse downstream targets of this complex to control unique aspects of the cell cycle. Our results in *Drosophila* wing discs support a model in which distinct Wts targets, Yki and Mud, function together to control tissue development

specifically through regulation of the rate and orientation of cell divisions, respectively (Figure 7G).

Wts serves as a negative regulator of cell proliferation yet promotes the activity of an essential spindle orientation pathway; thus, understanding how these events are coordinated with respect to cell cycle progression will be an important question to resolve. Interestingly, discs expressing both Mud^{RNAi} and Yki^{S168A} showed a reduction in overgrowth compared to Yki^{S168A} alone (Figure 7F), suggesting spindle misorientation suppresses tissue growth. Recent studies in *Drosophila* wing discs have shown that loss of genes involved in spindle assembly and orientation, including essential centrosomal proteins as well as Mud, can induce apoptosis resulting in stunted wing development [44, 48]. Our results suggest that loss of Mud can also suppress aberrant overgrowth under conditions of constitutive Yki activity. Whether spindle misorientation *per se* is sufficient to induce apoptosis in unclear, as defects in spindle assembly and chromosome segregation were also seen in these discs [48]. These results contrast with those obtained in certain model stem cell systems, in which spindle orientation defects are hypothesized to act synergistically with other overgrowth inducing mutations, including the those involved in the tumorigenesis process [4]. The evolutionarily-conserved nature of the Hippo pathway highlights the importance of continued unraveling of its role in both normal development as well as disease.

EXPERIMENTAL PROCEDURES

Fly stocks

The following stocks were obtained from the Bloomington Stock Center: VALIUM20 TRiP lines for mud^{RNAi} (stock# 35044), hpo^{RNAi} (stock# 33614), sav^{RNAi} (stock# 32965) and wts^{RNAi} (stock# 34064), *w; PUAS-yki.S168A.V5attP2* (stock# 28818), and the *UAS-Dcr-2.D1*, *w1118; PGawBnubbin-AC-62* (stock# 25754), *Ap-GAL4* (stock# 46223), and *En-GAL4* (stock# 35064). An additional "KK library" Wts^{RNAi} stock was obtained from the Vienna Drosophila Resource Center (VDRC; stock# 106174). The Mud and Yki double mutant was achieved using a *nub-GAL4/nub-GAL4;*mud^{RNAi}/mud^{RNAi} line generated using a *Cyo/Br;TM2/TM6* double balancer line (Richard M. Cripps, UNM). Generation of this line resulted in the loss of the *UAS-Dcr-2.D1* allele on the X-chromosome from the original *nub-GAL4* stock. Crossing this *nub-GAL4/nub-GAL4;*mud^{RNAi}/mud^{RNAi} line to *w; PUAS-yki.S168A.V5attP2* (for generation of Mud^{RNAi}/YkiS168A double mutants) thus resulted in the presence of two UAS sequence elements. Because single mutant crosses all retained the *UAS-Dcr-2.D1*, conditions in which *UAS-*Mud^{RNAi} or *UAS-YkiS168A* were expressed alone also contained two UAS elements, thereby ensuring wing disc growth phenotypes were not due to unequal copy numbers of UAS and GAL-4 elements.

Induced S2 cell polarity assay

Schneider S2 cells (Invitrogen; Carlsbad, CA, USA) were grown in Schneider's insect media supplemented with 10% heat-inactivated fetal bovine serum (SIM). Cells were passaged every 3–4 days and maintained at 25°C in the absence of CO_2. For transient transfections, 1×10^6 cells were placed in 6-well culture dishes for 30 minutes in 3 mL of SIM. Cells were then transfected with 0.05–1 μg total DNA using the Effectene® reagent

system according to manufacturer protocols (Qiagen, Germantown, MD, USA). Following 24–36 hour incubation, transgene expression was induced by the addition of $CuSO_4$ (500 μM) for 24 hours.

For the Echinoid-based 'induced polarity' assay, cells were harvested, pelleted, and resuspended in fresh SIM supplemented with $CuSO_4$. Cells were then placed in a new 6-well dish and rotated at ~175 RPM for 2–3 hours, allowing for stochastic cell collisions that lead to cell-cell contacts and cluster formation [10].

Immunostaining and imaging

Clustered cells (0.25 mL) were mixed with an 0.75 mL of fresh SIM in 24-well dishes containing 12 mm diameter round glass coverslips. Cells were incubated for 2–3 hours to allow for adherence to coverslips and to increase the percentage of mitotic cells. Cells were then fixed using a treatment of 4% paraformaldehyde (10 min) or ice-cold methanol (5 min). Cells were washed 3 times (5 min) with wash buffer (0.1% Triton X-100 in PBS), followed by a 1 hour incubation with block buffer (0.1% Triton X-100 and 1% BSA in PBS). Primary antibodies were then incubated with slides overnight at 4 °C. Following primary antibody incubation, slides were washed 3 times with block buffer. Secondary antibodies (Jackson Immuno Research) diluted 1:250 in block buffer were then added an incubated at room temperature for 2 hours. Antibodies were removed and slides were washed 4 times with wash buffer. Finally, coverslips were inverted and mounted using Vectashield® HardSet reagent (Vector Laboratories, Burlingame, CA, USA) and stored at 4 °C prior to imaging.

Antibodies used were as follows: mouse anti-FLAG (1:500; Sigma), rat anti-α-tubulin (1:500; Abcam), rabbit anti-Mud (1:1000), and rabbit anti-PH3 (1:2000, Abcam). γ-tubulin antibodies were obtained from Sigma (1:500, rabbit) and Abcam (1:1500, mouse). The anti-Yorkie and anti-Pins antibodies were generous gifts from Dr. Kenneth Irvine (Rutgers University, HHMI) and Dr. Chris Doe (University of Oregon, HHMI), respectively. Imaging was performed using a Nikon Eclipse Ti-S inverted fluorescence microscope and collected under oil immersion at 60× magnification. All secondary antibodies (preabsorbed and non-crossreactive) were obtained from Jackson ImmunoResearch and used at 1:250 dilutions.

RNAi design and treatment

RNAi primer designs were obtained using SnapDragon web-based service (http://www.flyrnai.org/snapdragon). Primer sets that amplify segments of ~200–600 base pairs within the coding sequence of desired targets were optimized for efficiency and specificity and designed with T7 promoter sequence recognition tags. Targeted sequences were designed to universally recognize all possible isoforms for desired transcript. PCR-amplified target sequences were transcribed to yield double-stranded RNA using the Megascript® T7 kit (Ambion, Austin, TX, USA) following the recommended protocol.

For RNAi treatment, S2 cells were seeded in 6-well dishes at 1×10^6 cells per well in 1 ml of serum-free Schneider growth media and incubated with 10 μg of respective RNAi. After 1 hour, 2 mL of serum-containing media were added and cells were incubated for an additional 3 days prior to subsequent assays.

Protein purification

Mud and Pins sequences were PCR amplified from an S2 cell cDNA library with BamHI/SalI (Mud) or BglII/SalI (Pins) restriction sites, enzyme digested, and ligated into pGEX and pBH4 plasmid backbones to generate GST and 6×His fusions, respectively. Mutation of Mud^{S1868} was carried out using standard PCR protocols. Plasmids were transformed into BL21(DE3) *E. coli* (Invitrogen) and cultures were grown at 37°C in standard LB supplemented with 100μg/mL ampicillin. At OD_{600} ~ 0.7, cultures were induced with 1mM Isopropyl β-D-1-thiogalactopyranoside and grown for an additional 4 hours. Protein purification was carried out using sequential NiNTA affinity, anion exchange, and size exclusion chromatographies. Proteins were concentrated using Vivaspin concentrators (Sigma Aldrich, St. Louis, MO), flash frozen in liquid nitrogen, and stored at −80°C in storage buffer (20mM Tris, pH 8, 100mM NaCl, and 2mM DTT).

GST pulldown assay

GST-tagged constructs were absorbed to glutathione agarose for 30 minutes at room temperature and subsequently washed 3 times with PBS. Subsequently, desired concentrations of prey proteins were added for 3 hours at 4°C with constant rocking in wash buffer (20mM Tris, pH 8; 100mM NaCl; 1mM DTT with 0.5% NP-40 or without for *in cis* Mud^{CC}/Mud^{PBD} binding experiments). Reactions were washed 4 times in respective wash buffers, and resolved samples were analyzed using coomassie blue staining.

In vitro kinase assays

Active, recombinant human LATS1 kinase domain (orthologous to *Drosophila* Warts), purified from Sf9 insect cells, was purchased from SignalChem. Purified Mud^{CC} constructs (50 μg) and LATS1 (1 μg) were diluted in ice-cold assay buffer (20mM Tris, pH 7.4, 100mM NaCl, 1mM DTT, 10mM MgCl2, and 10 μM ATP). To initiate reaction, [γ-32P]ATP (5 μCi) was added to each reaction and incubated at 30 °C for 30 minutes. Reactions were quenched by addition of SDS loading buffer. Samples were resolved by SDS-PAGE and dried gels were analyzed using Kodak BioMax MS film in a Konica SRX-101A developer.

Imaginal wing disc analysis

Imaginal wing discs were dissected from wandering third instar larvae in PBS. Discs were fixed in 4% paraformaldehyde at room temperature for 20 minutes with rocking. Following fixation, discs were washed three times in wash buffer (0.3% Triton X-100 in PBS) and then once at RT for 20 minutes with rocking. Discs were blocked in block buffer (0.3% Triton X-100 + 1% BSA in PBS) for 1 hour at room temperature. Phalloidin-568 (1:5) and primary antibodies in block buffer were incubated with rocking at 4°C for 24–48 hours. Discs were washed and treated with secondary antibodies in block buffer for 2 hours. Washed discs were mounted in Vectashield Mounting Medium for Fluorescence or 80% glycerol and stored at 4°C until imaged. Antibodies used were as follows: mouse γ-tubulin (1:500), rabbit Mud (1:1000), rabbit phosphohistone-H3 (1:1000), and rat Pins (1:500).

Supplementary Material

Refer to Web version on PubMed Central for supplementary material.

ACKNOWLEDGMENTS

This work was supported by a grants from the National Institutes of Health: R01-GM108756 (C.A.J.) and R25-HG007630 (D.S. via UNM Post-baccalaureate Research and Education Program).

REFERENCES

1. Cabernard C, Doe CQ. Apical/basal spindle orientation is required for neuroblast homeostasis and neuronal differentiation in Drosophila. Developmental cell. 2009; 17:134–141. [PubMed: 19619498]
2. Lee CY, Andersen RO, Cabernard C, Manning L, Tran KD, Lanskey MJ, Bashirullah A, Doe CQ. Drosophila Aurora-A kinase inhibits neuroblast self-renewal by regulating aPKC/Numb cortical polarity and spindle orientation. Genes & development. 2006; 20:3464–3474. [PubMed: 17182871]
3. Lechler T, Fuchs E. Asymmetric cell divisions promote stratification and differentiation of mammalian skin. Nature. 2005; 437:275–280. [PubMed: 16094321]
4. Gonzalez C. Spindle orientation, asymmetric division and tumour suppression in Drosophila stem cells. Nature reviews. Genetics. 2007; 8:462–472. [PubMed: 17510666]
5. Bellaiche Y, Radovic A, Woods DF, Hough CD, Parmentier ML, O'Kane CJ, Bryant PJ, Schweisguth F. The Partner of Inscuteable/Discs-large complex is required to establish planar polarity during asymmetric cell division in Drosophila. Cell. 2001; 106:355–366. [PubMed: 11509184]
6. Colombo K, Grill SW, Kimple RJ, Willard FS, Siderovski DP, Gonczy P. Translation of polarity cues into asymmetric spindle positioning in Caenorhabditis elegans embryos. Science. 2003; 300:1957–1961. [PubMed: 12750478]
7. Du Q, Stukenberg PT, Macara IG. A mammalian Partner of inscuteable binds NuMA and regulates mitotic spindle organization. Nature cell biology. 2001; 3:1069–1075. [PubMed: 11781568]
8. Lee CY, Robinson KJ, Doe CQ. Lgl, Pins and aPKC regulate neuroblast self-renewal versus differentiation. Nature. 2006; 439:594–598. [PubMed: 16357871]
9. Schaefer M, Petronczki M, Dorner D, Forte M, Knoblich JA. Heterotrimeric G proteins direct two modes of asymmetric cell division in the Drosophila nervous system. Cell. 2001; 107:183–194. [PubMed: 11672526]
10. Johnston CA, Hirono K, Prehoda KE, Doe CQ. Identification of an Aurora-A/PinsLINKER/Dlg spindle orientation pathway using induced cell polarity in S2 cells. Cell. 2009; 138:1150–1163. [PubMed: 19766567]
11. Lu MS, Johnston CA. Molecular pathways regulating mitotic spindle orientation in animal cells. Development. 2013; 140:1843–1856. [PubMed: 23571210]
12. Kotak S, Busso C, Gonczy P. Cortical dynein is critical for proper spindle positioning in human cells. The Journal of cell biology. 2012; 199:97–110. [PubMed: 23027904]
13. Bowman SK, Neumuller RA, Novatchkova M, Du Q, Knoblich JA. The Drosophila NuMA Homolog Mud regulates spindle orientation in asymmetric cell division. Developmental cell. 2006; 10:731–742. [PubMed: 16740476]
14. Siller KH, Cabernard C, Doe CQ. The NuMA-related Mud protein binds Pins and regulates spindle orientation in Drosophila neuroblasts. Nature cell biology. 2006; 8:594–600. [PubMed: 16648843]
15. Kiyomitsu T, Cheeseman IM. Chromosome- and spindle-pole-derived signals generate an intrinsic code for spindle position and orientation. Nature cell biology. 2012; 14:311–317. [PubMed: 22327364]
16. Kotak S, Busso C, Gonczy P. NuMA phosphorylation by CDK1 couples mitotic progression with cortical dynein function. The EMBO journal. 2013; 32:2517–2529. [PubMed: 23921553]

17. Zhao B, Tumaneng K, Guan KL. The Hippo pathway in organ size control, tissue regeneration and stem cell self-renewal. Nature cell biology. 2011; 13:877–883. [PubMed: 21808241]
18. Hotz M, Barral Y. The Mitotic Exit Network: new turns on old pathways. Trends in cell biology. 2014; 24:145–152. [PubMed: 24594661]
19. Menssen R, Neutzner A, Seufert W. Asymmetric spindle pole localization of yeast Cdc15 kinase links mitotic exit and cytokinesis. Current biology : CB. 2001; 11:345–350. [PubMed: 11267871]
20. Hotz M, Leisner C, Chen D, Manatschal C, Wegleiter T, Ouellet J, Lindstrom D, Gottschling DE, Vogel J, Barral Y. Spindle pole bodies exploit the mitotic exit network in metaphase to drive their age-dependent segregation. Cell. 2012; 148:958–972. [PubMed: 22385961]
21. Guo C, Tommasi S, Liu L, Yee JK, Dammann R, Pfeifer GP. RASSF1A is part of a complex similar to the Drosophila Hippo/Salvador/Lats tumor-suppressor network. Current biology : CB. 2007; 17:700–705. [PubMed: 17379520]
22. Mardin BR, Agircan FG, Lange C, Schiebel E. Plk1 controls the Nek2A–PP1gamma antagonism in centrosome disjunction. Current biology : CB. 2011; 21:1145–1151. [PubMed: 21723128]
23. Mardin BR, Lange C, Baxter JE, Hardy T, Scholz SR, Fry AM, Schiebel E. Components of the Hippo pathway cooperate with Nek2 kinase to regulate centrosome disjunction. Nature cell biology. 2010; 12:1166–1176. [PubMed: 21076410]
24. Morisaki T, Hirota T, Iida S, Marumoto T, Hara T, Nishiyama Y, Kawasuzi M, Hiraoka T, Mimori T, Araki N, et al. WARTS tumor suppressor is phosphorylated by Cdc2/cyclin B at spindle poles during mitosis. FEBS letters. 2002; 529:319–324. [PubMed: 12372621]
25. Toji S, Yabuta N, Hosomi T, Nishihara S, Kobayashi T, Suzuki S, Tamai K, Nojima H. The centrosomal protein Lats2 is a phosphorylation target of Aurora-A kinase. Genes to cells : devoted to molecular & cellular mechanisms. 2004; 9:383–397. [PubMed: 15147269]
26. Yabuta N, Mukai S, Okada N, Aylon Y, Nojima H. The tumor suppressor Lats2 is pivotal in Aurora A and Aurora B signaling during mitosis. Cell cycle. 2011; 10:2724–2736. [PubMed: 21822051]
27. Izumi Y, Ohta N, Hisata K, Raabe T, Matsuzaki F. Drosophila Pins-binding protein Mud regulates spindle-polarity coupling and centrosome organization. Nature cell biology. 2006; 8:586–593. [PubMed: 16648846]
28. Hergovich A, Stegert MR, Schmitz D, Hemmings BA. NDR kinases regulate essential cell processes from yeast to humans. Nature reviews. Molecular cell biology. 2006; 7:253–264. [PubMed: 16607288]
29. Emoto K, He Y, Ye B, Grueber WB, Adler PN, Jan LY, Jan YN. Control of dendritic branching and tiling by the Tricornered-kinase/Furry signaling pathway in Drosophila sensory neurons. Cell. 2004; 119:245–256. [PubMed: 15479641]
30. Huang J, Wu S, Barrera J, Matthews K, Pan D. The Hippo signaling pathway coordinately regulates cell proliferation and apoptosis by inactivating Yorkie, the Drosophila Homolog of YAP. Cell. 2005; 122:421–434. [PubMed: 16096061]
31. Wu S, Huang J, Dong J, Pan D. hippo encodes a Ste-20 family protein kinase that restricts cell proliferation and promotes apoptosis in conjunction with salvador and warts. Cell. 2003; 114:445–456. [PubMed: 12941273]
32. Oh H, Irvine KD. In vivo regulation of Yorkie phosphorylation and localization. Development. 2008; 135:1081–1088. [PubMed: 18256197]
33. Hao Y, Chun A, Cheung K, Rashidi B, Yang X. Tumor suppressor LATS1 is a negative regulator of oncogene YAP. The Journal of biological chemistry. 2008; 283:5496–5509. [PubMed: 18158288]
34. Yang CH, Lambie EJ, Snyder M. NuMA: an unusually long coiled-coil related protein in the mammalian nucleus. The Journal of cell biology. 1992; 116:1303–1317. [PubMed: 1541630]
35. Chiyoda T, Sugiyama N, Shimizu T, Naoe H, Kobayashi Y, Ishizawa J, Arima Y, Tsuda H, Ito M, Kaibuchi K, et al. LATS1/WARTS phosphorylates MYPT1 to counteract PLK1 and regulate mammalian mitotic progression. The Journal of cell biology. 2012; 197:625–641. [PubMed: 22641346]
36. Zhu J, Wen W, Zheng Z, Shang Y, Wei Z, Xiao Z, Pan Z, Du Q, Wang W, Zhang M. LGN/mInsc and LGN/NuMA complex structures suggest distinct functions in asymmetric cell division for the

Par3/mInsc/LGN and Galphai/LGN/NuMA pathways. Molecular cell. 2011; 43:418–431. [PubMed: 21816348]

37. Feng Y, Irvine KD. Fat and expanded act in parallel to regulate growth through warts. Proceedings of the National Academy of Sciences of the United States of America. 2007; 104:20362–20367. [PubMed: 18077345]
38. Grusche FA, Richardson HE, Harvey KF. Upstream regulation of the hippo size control pathway. Current biology : CB. 2010; 20:R574–R582. [PubMed: 20619814]
39. Mao Y, Rauskolb C, Cho E, Hu WL, Hayter H, Minihan G, Katz FN, Irvine KD. Dachs: an unconventional myosin that functions downstream of Fat to regulate growth, affinity and gene expression in Drosophila. Development. 2006; 133:2539–2551. [PubMed: 16735478]
40. Mao Y, Tournier AL, Bates PA, Gale JE, Tapon N, Thompson BJ. Planar polarization of the atypical myosin Dachs orients cell divisions in Drosophila. Genes & development. 2011; 25:131–136. [PubMed: 21245166]
41. Mao Y, Tournier AL, Hoppe A, Kester L, Thompson BJ, Tapon N. Differential proliferation rates generate patterns of mechanical tension that orient tissue growth. The EMBO journal. 2013; 32:2790–2803. [PubMed: 24022370]
42. Repiso A, Bergantinos C, Serras F. Cell fate respecification and cell division orientation drive intercalary regeneration in Drosophila wing discs. Development. 2013; 140:3541–3551. [PubMed: 23903186]
43. Rauskolb C, Sun S, Sun G, Pan Y, Irvine KD. Cytoskeletal tension inhibits Hippo signaling through an Ajuba-Warts complex. Cell. 2014; 158:143–156. [PubMed: 24995985]
44. Nakajima Y, Meyer EJ, Kroesen A, McKinney SA, Gibson MC. Epithelial junctions maintain tissue architecture by directing planar spindle orientation. Nature. 2013; 500:359–362. [PubMed: 23873041]
45. Baena-Lopez LA, Baonza A, Garcia-Bellido A. The orientation of cell divisions determines the shape of Drosophila organs. Current biology : CB. 2005; 15:1640–1644. [PubMed: 16169485]
46. Bell GP, Fletcher GC, Brain R, Thompson BJ. Aurora kinases phosphorylate Lgl to induce mitotic spindle orientation in Drosophila epithelia. Current biology : CB. 2015; 25:61–68. [PubMed: 25484300]
47. Segalen M, Johnston CA, Martin CA, Dumortier JG, Prehoda KE, David NB, Doe CQ, Bellaiche Y. The Fz-Dsh planar cell polarity pathway induces oriented cell division via Mud/NuMA in Drosophila and zebrafish. Developmental cell. 2010; 19:740–752. [PubMed: 21074723]
48. Poulton JS, Cuningham JC, Peifer M. Acentrosomal Drosophila epithelial cells exhibit abnormal cell division, leading to cell death and compensatory proliferation. Developmental cell. 2014; 30:731–745. [PubMed: 25241934]
49. Siller KH, Doe CQ. Spindle orientation during asymmetric cell division. Nature cell biology. 2009; 11:365–374. [PubMed: 19337318]
50. Carmena A, Makarova A, Speicher S. The Rap1-Rgl-Ral signaling network regulates neuroblast cortical polarity and spindle orientation. The Journal of cell biology. 2011; 195:553–562. [PubMed: 22084305]
51. Wee B, Johnston CA, Prehoda KE, Doe CQ. Canoe binds RanGTP to promote Pins(TPR)/Mud-mediated spindle orientation. The Journal of cell biology. 2011; 195:369–376. [PubMed: 22024168]
52. Mauser JF, Prehoda KE. Inscuteable regulates the Pins-Mud spindle orientation pathway. PloS one. 2012; 7:e29611. [PubMed: 22253744]
53. Wang C, Li S, Januschke J, Rossi F, Izumi Y, Garcia-Alvarez G, Gwee SS, Soon SB, Sidhu HK, Yu F, et al. An ana2/ctp/mud complex regulates spindle orientation in Drosophila neuroblasts. Developmental cell. 2011; 21:520–533. [PubMed: 21920316]
54. Hergovich A. Regulation and functions of mammalian LATS/NDR kinases: looking beyond canonical Hippo signalling. Cell & bioscience. 2013; 3:32. [PubMed: 23985307]

HIGHLIGHTS

- Warts directly phosphorylates Mud to regulate Pins binding *in vitro*
- Warts is necessary for cortical localization of Mud to a polarized Pins cue
- Warts promotes spindle orientation in *Drosophila* imaginal wing disc epithelia
- Warts-mediated spindle orientation does not require its canonical effector, Yorkie

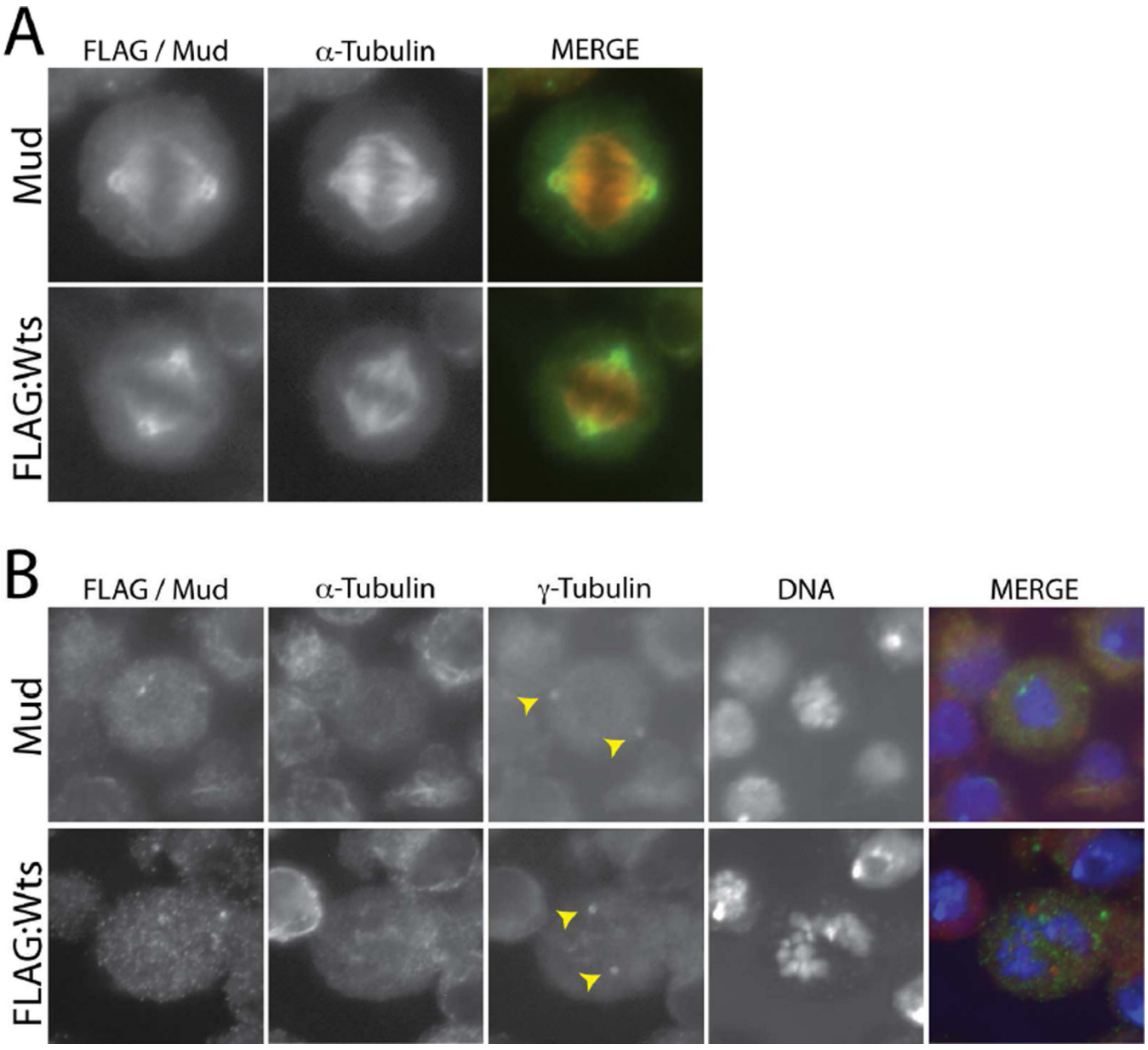

Figure 1. Warts localizes to mitotic spindle poles in mitotic S2 cells

(A) Cells were transfected with full-length Warts tagged with an N-terminal FLAG epitope sequence (FLAG:Wts) and stained with antibodies against FLAG and α-tubulin. To visualize endogenous Mud, untransfected cells were stained with an α-tubulin and Mud antibodies. **(B)** To depolymerize spindle microtubules, cells were treated with colchicine (12.5 μM) for 2 hours prior to fixation and antibody staining. Yellow arrowheads indicate both γ-tubulin-positive centrosomes, to which neither Wts nor Mud show significant localization. α-tubulin staining indicates successful depolymerization of spindle microtubules; note this channel is not shown in the merge panel.

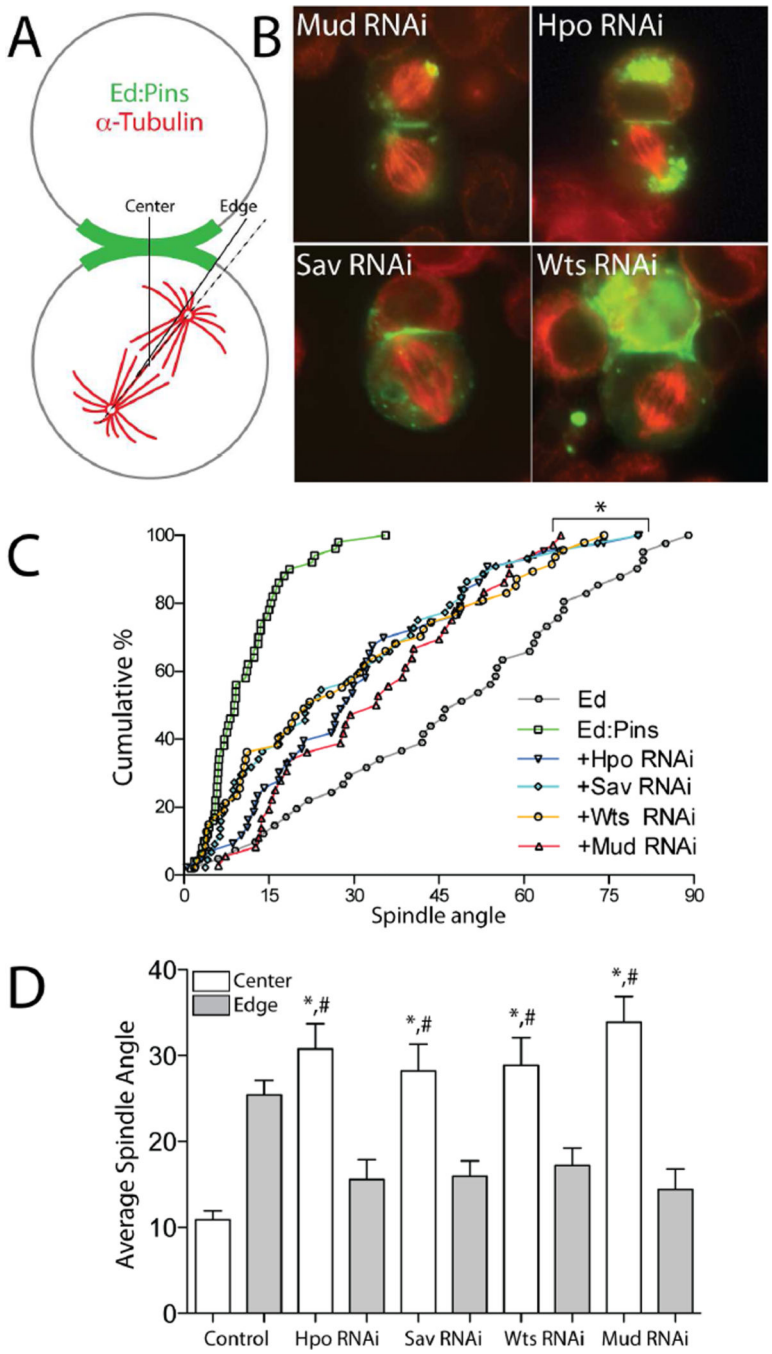

Figure 2. The core Hippo kinase complex is required for robust Pins-mediated spindle orientation in polarized S2 cells

(A) Schematic overview of induced polarity assay. Cells are transfected with Pins fused to the truncated intracellular C-terminus of the adhesion protein Echnoid (Ed), which also contains GFP for visualization. Cell adhesion induces polarized Ed-based crescents, relative to which mitotic spindle orientation is measured. **(B)** S2 cells were transfected with Ed:GFP:Pins and subsequently treated with dsRNAi against indicated protein. Cells were fixed and stained with an α-tubulin antibody. In addition to the contact-induced cortical

crescent, Ed:GFP:Pins often forms cytoplasmic puncta that can accumulate at peri-centrosomal regions. This localization can still occur in the presence of each RNAi treatment, suggesting that neither the Hippo complex nor Mud are required for this non-cortical localization. Also, previous studies have shown spindle orientation to be independent of the amount of puncta present [10]. **(C)** Spindle angles from at least 30 individual cells for each genotype are plotted as the cumulative percentage of cells at or below a given angle of spindle orientation. Each RNAi causes a phenotype intermediate between fully active Ed:Pins and the Ed alone negative control. Each RNAi condition was statistically different from both Ed and Ed:Pins but not one another (*, $p < 0.05$ ANOVA with Tukey's *post-hoc* test). **(D)** Spindle angles were measured relative to the Ed:Pins crescent edge (*grey filled bars*) and center (*open bars*) for each condition. Fully active Ed:Pins (Control) positions spindles more closely to the center, whereas Hpo, Sav, and Wts RNAi preferentially orient spindles to the edge similar to Mud RNAi. *, $p < 0.05$ for 'center' versus 'edge' values within respective genotypes; #, $p<0.05$ for given RNAi 'center' compared to Control 'center', ANOVA followed by Tukey's *post-hoc* test. The absence or presence of peri-centrosomal Ed:Pins puncta was similar across all conditions examined and did not show any significant correlation with spindle angle measurements, demonstrating they neither interfere with nor contribute to the spindle orientation process. See also Figure S1.

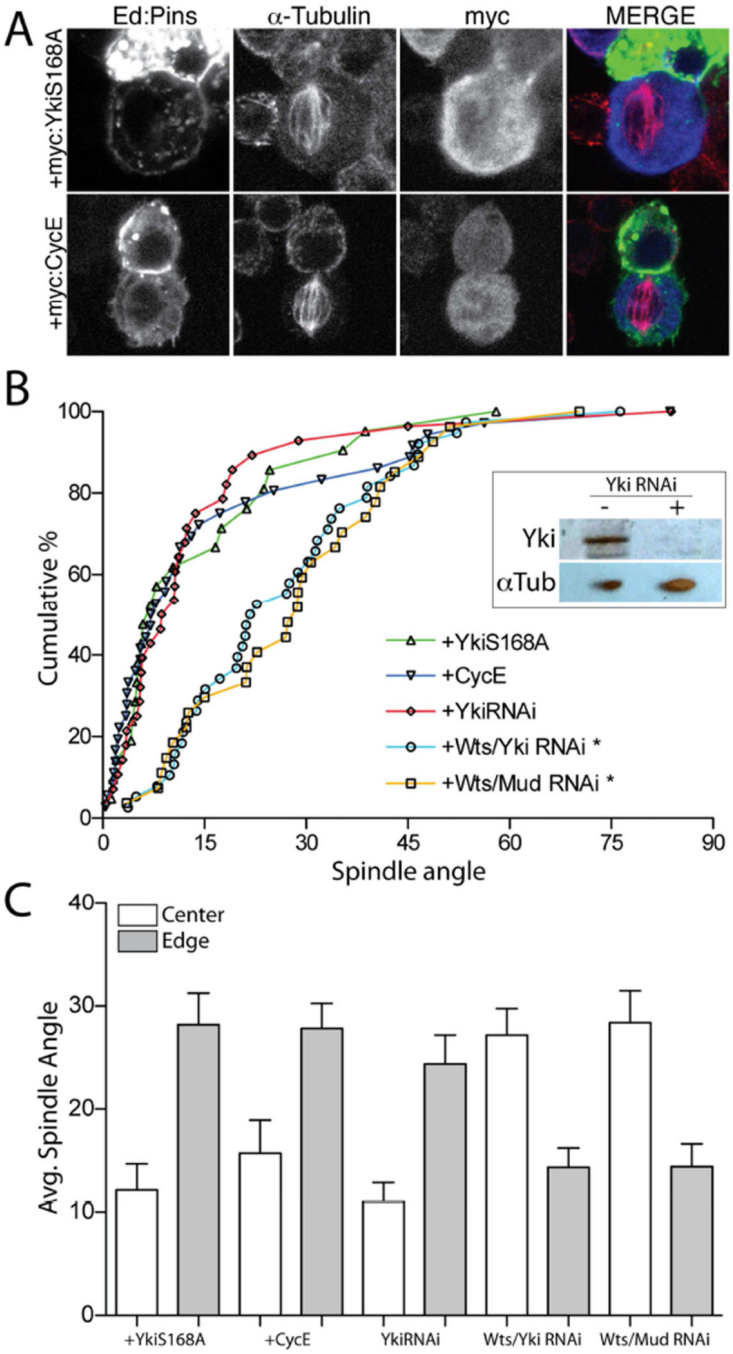

Figure 3. Hippo signaling acts independently of its canonical effector, Yorkie, to control S2 cell spindle orientation

(A) Cells were transfected with Ed:GFP:Pins together with either Yorkie-S168A (YkiS168A) or cyclin-E (CycE) as N-terminal c-myc tag fusion constructs. Cells were fixed and stained with antibodies against α-tubulin and the c-myc epitope. **(B)** Cumulative percentage plots for indicated genotypes. Neither CycE nor YkiS168A affect Ed:Pins function; RNAi against Yki was also without effect. Combined treatment of Wts and Yki RNAi or Wts and Mud RNAi resulted in spindle orientation similar to either Wts or Mud

RNAi alone. *Inset*: western blot (20 μg total S2 cell lysate protein) indicating robust knockdown of Yki protein expression in cells treated with Yki^{RNAi}. *, $p < 0.05$ compared to Ed:Pins, ANOVA followed by Tukey's *post-hoc* test. **(C)** Spindle angles were measured relative to the Ed:Pins crescent edge (*grey filled bars*) and center (*open bars*) for each condition. In each genotype, edge and center measurements were statistically separated, $p < 0.05$, ANOVA followed by Tukey's *post-hoc* test.

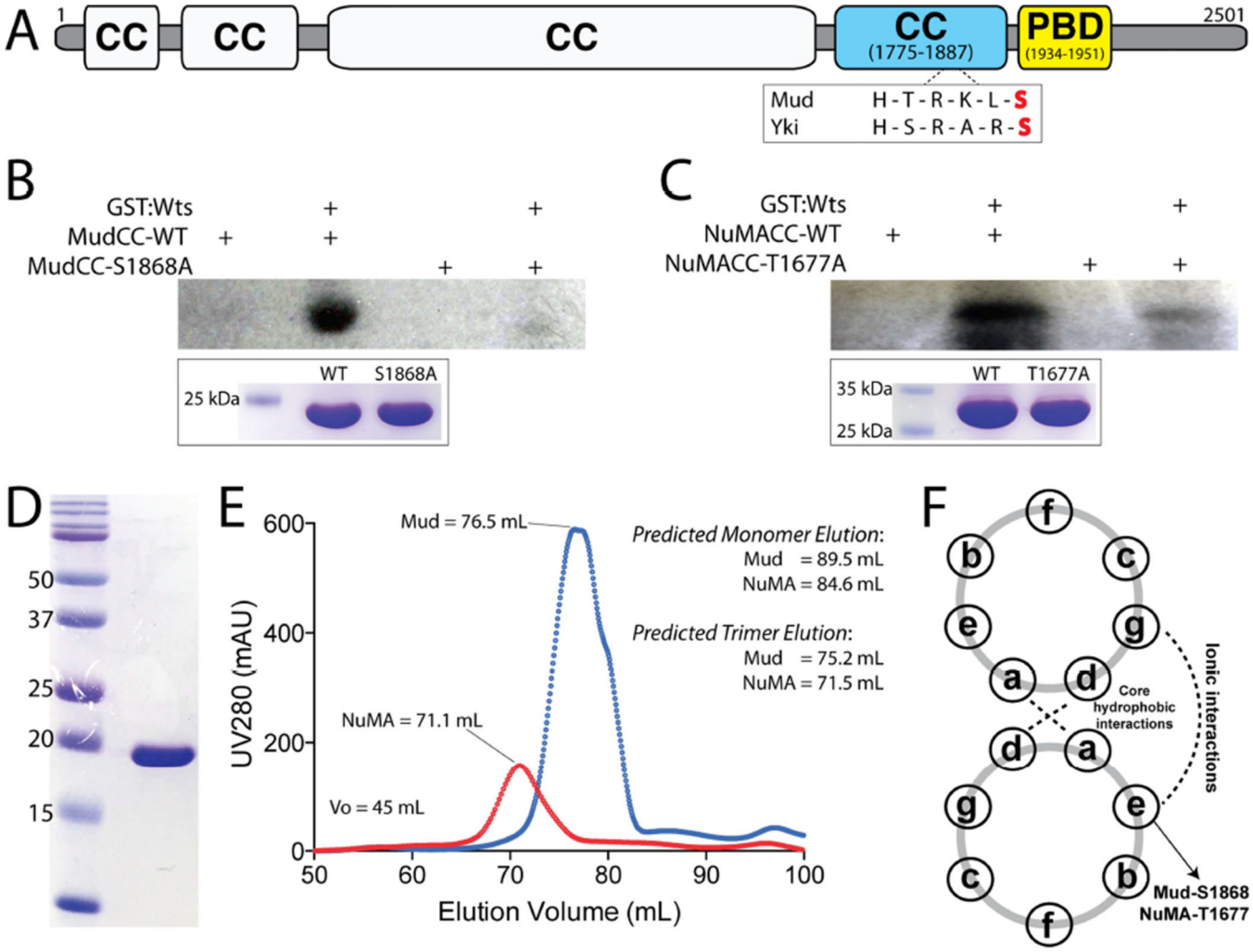

Figure 4. Warts directly phosphorylates Mud within its C-terminal coiled-coil domain

(A) The domain architecture of Mud consists primarily of coiled coil (CC) domains. The most C-terminal of these (Mud^{CC}; *blue*) contains a single consensus phosphorylation motif for Wts kinase that closely resembles that found in Yki. Immediately following this domain is the minimal Pins-binding domain (Mud^{PBD}; *yellow*). **(B)** Mud^{CC}, wild-type (MudCC-WT) or a single S1868A mutant (MudCC-S1868A), were incubated in the absence or presence of GST:Wts kinase together with [γ-32P]-ATP. Radioactive phosphate incorporation was assessed by autoradiography using Kodak BioMax-MS radioisotope film. *Inset below*: Coomassie stain of reaction inputs showing equal levels of Mud protein between phosphorylation conditions. **(C)** Identical experiments carried out with the $NuMA^{CC}$ domain and the corresponding T1677A mutant. **(D)** Coomassie stained gel indicating homogenous purity of the Mud^{CC} protein purification. **(E)** Both Mud^{CC} and $NuMA^{CC}$ domains elute from a size-exclusion column at volumes consistent with trimers. Predicted elution volumes were calculated from a standard curve performed on the HiLoad Superdex 200 column (GE Healthcare). **(F)** Schematic of coiled-coil heptad repeat residue interactions. Both S1868 in Mud^{CC} and T1677 in $NuMA^{CC}$ are predicted to reside at 'e' positions, which participate in ionic interactions in an ideal coiled-coil. See also Figure S2.

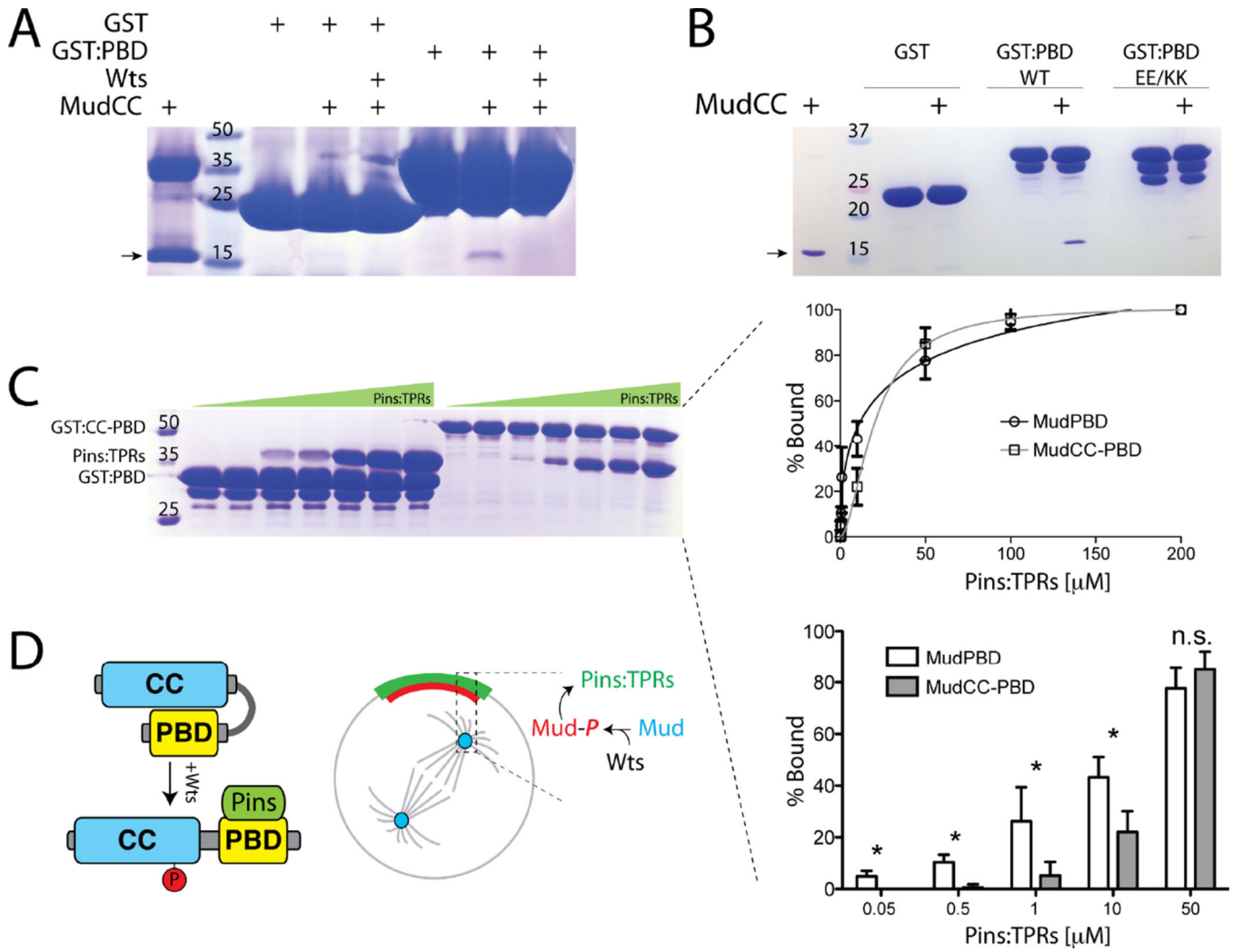

Figure 5. Mud phosphorylation modulates its direct interaction with Pins

(A) Mud^{CC} was incubated in the absence or presence of Wts kinase to allow phosphorylation. Proteins were then incubated with GST or GST fused to Mud^{PBD} (GST:PBD), resolved by SDS-PAGE and coomassie stained to determine bound proteins. Wts inhibits the ability of GST:PBD to co-precipitate Mud^{CC}. The higher molecular weight band in lane 1 is an impurity that sometimes proved difficult to remove during Mud^{CC} purification. **(B)** Mud^{CC} was incubated with GST or GST:PBD, either as wild-type (WT) sequence or a E1939K/E1941K double mutant (EE/KK). The mutant PBD is severely impaired in its ability to bind Mud^{CC}. The arrow in panels A and B indicates Mud^{CC}**(C)** Mud^{PBD} alone or in tandem with the coiled-coil ($Mud^{CC\text{-}PBD}$) were fused to GST and incubated with increasing concentrations of the TPR domains of Pins (Pins:TPRs). Bands representing Pins:TPRs were quantified using densitometry analysis (ImageJ) and plotted as percent bound (*right insets*). Inclusion of the coiled-coil domain (*i.e.* $Mud^{CC\text{-}PBD}$) significantly reduced interaction with Pins:TPRs at concentrations up to 10 μM. **(D)** Model for Wts-mediated Mud regulation. Self-association between Mud^{CC} and Mud^{PBD} domains prevents Pins binding at low concentrations. Wts phosphorylation of Mud^{CC} allows for high

affinity Pins binding at the cell cortex. Whether the cortical and spindle pole Mud pools are directly connected remains to be determined, as is the precise mechanism for cortical Mud translocation. Statistical analyses were performed using ANOVA with Tukey's *post-hoc* test.

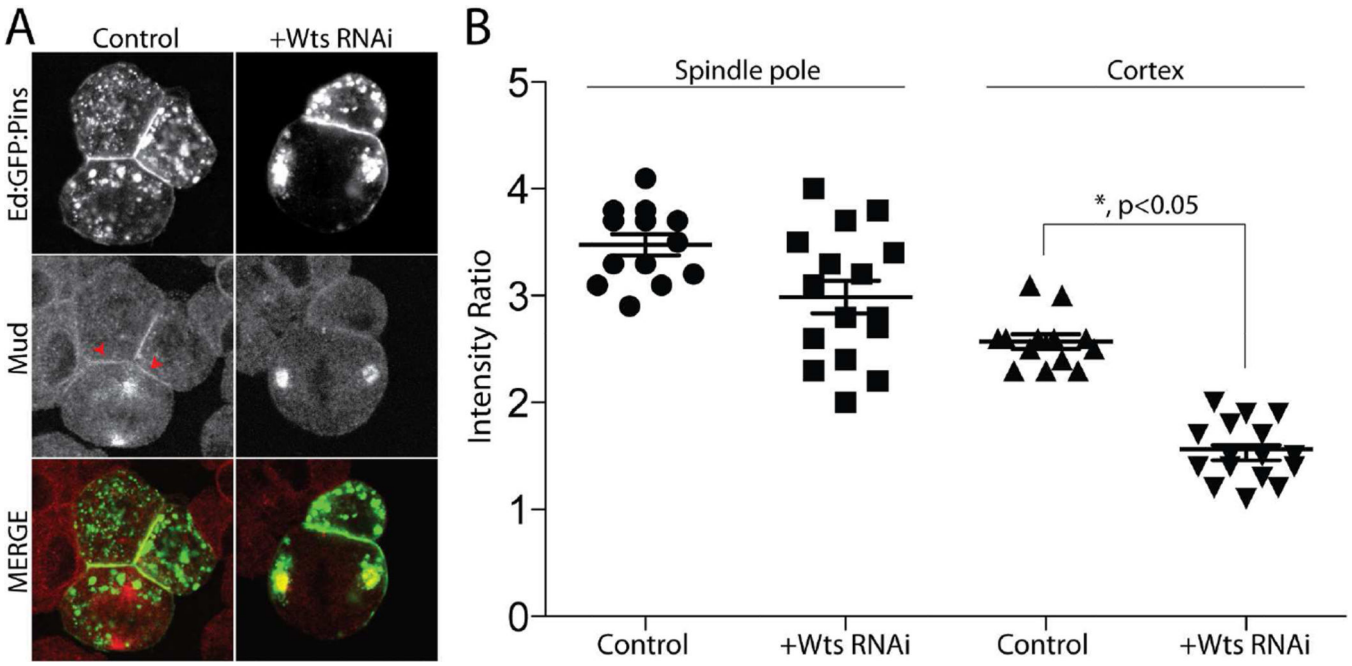

Figure 6. Warts kinase is dispensable for spindle pole Mud localization but necessary for its cortical association with Pins

(A) Cells were transfected with Ed:GFP:Pins and treated without (Control) or with RNAi against Warts (+Wts RNAi). Cells were fixed and stained for endogenous Mud. **(B)** The relative intensities of cortical and spindle pole localized Mud were calculated relative to cytoplasmic signal using ImageJ software. Wts^{RNAi} reduces cortical Mud accumulation without affecting its localization to spindle poles. Statistical analysis was performed using ANOVA with Tukey's *post-hoc* test.

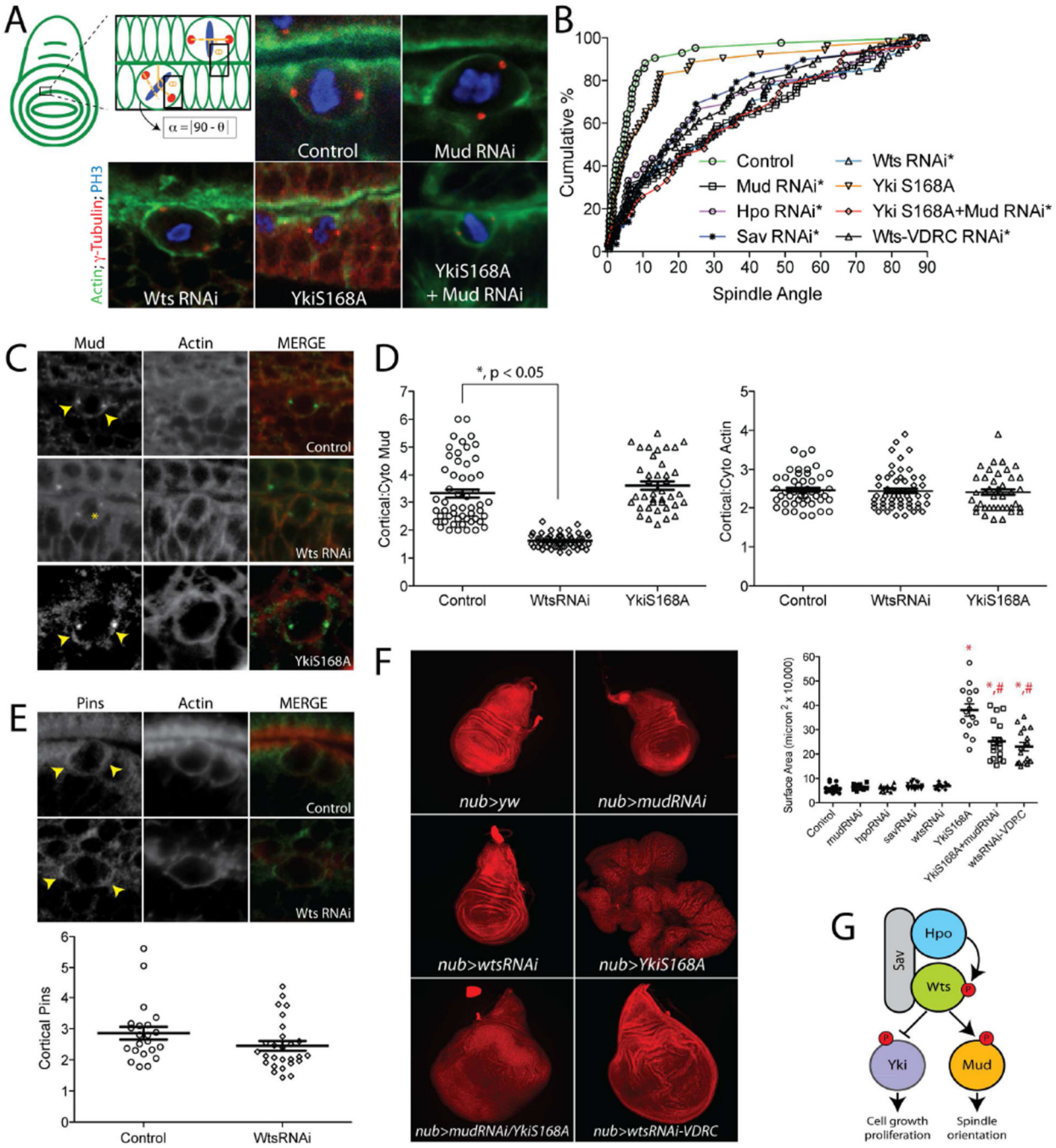

Figure 7. Warts is required for cortical Mud localization and spindle orientation in wing imaginal disc epithelial cells

(A) Spindle orientation in individual epithelial cells of third instar larval imaginal wing discs were measured relative to actin rich folds. Representative images show spindle positioning in indicated genotypes. Discs were dissected and stained with antibodies against γ-tubulin (to mark centrosomes), phosphohistone-H3 (PH3), and phalloidin (to label actin). **(B)** Cumulative percentage plots for all collected measurements. Expression of Yki^{S168A} does not significantly alter spindle orientation, whereas RNAi against Hpo, Sav, or Wts results in

nearly identical loss of spindle orientation as Mud^{RNAi} expression. A second 'Wts-VDRC' RNAi causes statistically equal spindle orientation defects. Asterisks indicate conditions significantly different from control. **(C)** Expression of Wts^{RNAi}, but not Yki^{S168A}, causes loss of cortical Mud accumulation (*yellow arrowhead indicates sharp cortical Mud signal; yellow asterisk indicates delocalized Mud signal*). **(D)** Cortical Mud and actin intensity ratios relative to cytoplasmic signal were calculated for each condition. **(E)** Pins localizes to the cell cortex of dividing wing disc cells with preferential accumulation near spindle poles (*yellow arrowheads*). Quantifications are shown below images: in contrast to Mud, expression of Wts^{RNAi} does not significantly affect cortical Pins localization. **(F)** Whole wing discs from L3 staged larvae were imaged at identical magnification for each genotype and maximum intensity projections of z-stacks were generated in Zen software (Carl Zeiss). Although neither Mud^{RNAi} nor Hpo, Sav, or Wts^{RNAi} caused dramatic effects on disc size, expression of Yki^{S168A} induced significant overgrowth. Animals expressing both Mud^{RNAi} and Yki^{S168A} had a significantly reduced overgrowth compared to Yki^{S168A} alone. Discs from the alternate Wts-VDRC animals were overgrown to a similar degree as double mutant discs. *, $p < 0.05$ compared to Control; #, $p < 0.05$ compared to YkiS168A, ANOVA with Tukey's *post-hoc* test. **(G)** Model for dual Warts functionality in wing discs: an inhibitory phosphorylation of Yki restricts cell proliferation, whereas an activating phosphorylation of Mud promotes proper spindle orientation. See also Figures S3 and S4.